Journal of Alloys and Compounds 509 (2011) 7109–7115

Contents lists available at ScienceDirect

Journal of Alloys and Compounds

journal homepage: www.elsevier.com/locate/jallcom

Analysis of controlled-mechanism of grain growth in undercooled Fe–Cu alloy

Zheng Chen [a,*], Feng Liu [b], Xiaoqin Yang [a], Chengjin Shen [a], Yu Fan [a]

[a] School of Material Science and Engineering, China University of Mining and Technology, Xuzhou, Jiangsu 221008, PR China
[b] State Key Laboratory of Solidification Processing, Northwestern Polytechnical University, Xi'an, Shaanxi 710072, PR China

ARTICLE INFO

Article history:
Received 20 February 2011
Received in revised form 28 March 2011
Accepted 2 April 2011
Available online 9 April 2011

Keywords:
Undercooling
Grain growth
Segregation
Stabilization

ABSTRACT

An analysis of controlled-mechanism of grain growth in the undercooled Fe–4 at.% Cu immiscible alloy was presented. Grain growth behavior of the single-phase supersaturated granular grains prepared in Fe–Cu immiscible alloy melt was investigated by performing isothermal annealings at 500–800 °C. The thermo-kinetic model [Chen et al., Acta Mater. 57 (2009) 1466] applicable for nano-scale materials was extended to the system of micro-scale undercooled Fe–4 at.% Cu alloy. In comparison of pure kinetic model, pure thermodynamic model and the extended thermo-kinetic model, two characteristic annealing time (t_1 and t_2) were determined. The controlled-mechanism of grain growth in undercooled Fe–Cu alloy was proposed, including a mainly kinetic-controlled process ($t \le t_1$), a transition from kinetic-mechanism to thermodynamic-mechanism ($t_1 < t < t_2$) and purely thermodynamic-controlled process ($t \ge t_2$).

1. Introduction

The study of granular materials (e.g. Fe–Cu alloy) consisting of ferromagnetic particles has become very useful in hi-tech applications, mainly due to the occurrence of giant magnetoresistance effects in such materials [1]. Numerous studies on Fe–Cu granular alloys prepared by sputtering [2] or melt-spinning [3] techniques have been carried out. The single-phase supersaturated granular grains for the Fe–4 at.% Cu immiscible alloy have been prepared applying highly undercooled solidification technique [4]. Subjected to low undercooling, a coarse dendritic pattern was obtained, where both Cu solute segregation and dot substructure can be observed. If the initial melt undercooling ΔT was higher than a critical value ΔT^*, a typical granular structure was formed, where the dot substructure still existed because of post-recalescence effect [4]. Therefore, only if both sufficiently high undercooling and rapid quenching immediately after recalescence were carried out, a single-phase supersaturated granular grains could be obtained, where the Cu precipitation and the dot substructure were suppressed [4].

The highly undercooled rapid solidification is a non-equilibrium solidification which changes the growth velocity and solidification behavior [4,5], thus inducing that the as-solidified Fe–Cu granular grains are unstable because of the non-equilibrium effects. It is very important to investigate how to obtain the microstructures with higher stabilization to extend their application.

Stability of the as-prepared alloys with respect to grain growth was discussed controversially. Some authors [6–8] claimed that solute drag (i.e. kinetic effect) by alloy or impurity atoms reduced the mobility of the grain boundaries (GBs) whereas others attributed it to a vanishing GB energy σ_b (i.e. thermodynamic effect) [9–12]. As is well known, for grain growth, the kinetic model points to the evolution process of grain size, whereas, the thermodynamic model favors the effect of GB energy decreasing with GB segregation. In other words, the stabilized grain size cannot be determined by the kinetic models, and the evolution of grain size cannot be described by the thermodynamic approaches [13–15]. Therefore, the thermo-kinetic model which combines the effect of kinetics and thermodynamics is more appropriate for describing the process of grain growth. Departing from Borisov's equation [16], Chen et al. [14] derived a thermo-kinetic model for the evolution of grain size by incorporation of the reduced GB energy into the parabolic kinetics of grain growth. Furthermore, a thermo-kinetic description was performed by Gong et al. [17] for nano-scale grain growth through analysis of the effect of GB segregation on the initial GB excess amount, Γ_b.

This paper presented a mechanism of a single-phase supersaturated granular grains formation through an analysis of the effects of absolute solute trapping and δ/γ massive transformation after recalescence by taking Fe–4 at.% Cu immiscible alloy as the experimental alloy. The thermo-kinetic model considering the mixed effects of solute drag and reduced GB energy was extended to describe micro-scale grain growth and then was applied to analyze the grain growth in undercooled Fe–Cu alloy. Finally, based on two characteristic annealing time (t_1 and t_2), the controlled-mechanism of grain size evolution was discussed.

* Corresponding author. Tel.: +86 0516 83897715; fax: +86 0516 83591870.
E-mail address: chenzheng1218@163.com (Z. Chen).

0925-8388/$ – see front matter © 2011 Elsevier B.V. All rights reserved.
doi:10.1016/j.jallcom.2011.04.014

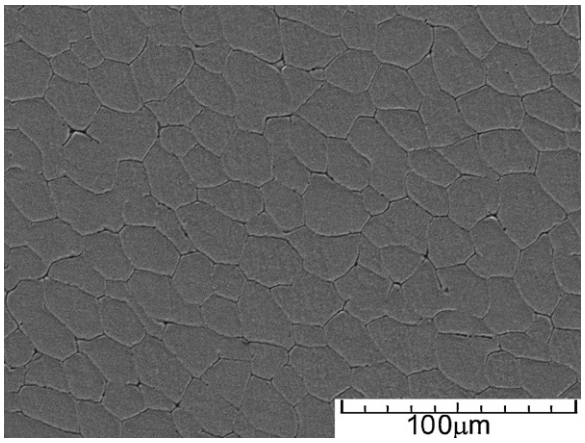

Fig. 1. Microstructure of the as-solidified single-phase supersaturated granular grains in undercooled Fe–4 at.% Cu alloy (with undercooling at 210 K).

2. Experimental details

Applying glass fluxing combined with cyclic superheating and rapid quenching into the Ga–In–Sn bath after recalescence, a homogeneous supersaturated granular grain was obtained for the undercooled Fe–4 at.% Cu alloy melts. The detailed experimental procedure is available in Ref. [4].

To investigate the behavior of grain growth and solute segregation, isothermal anneals at different temperatures (500–800 °C) were conducted in a vacuum-electrical-resistance furnace under the protection of Ar atmosphere. The annealing temperature was selected below the eutectoid point (≈850 °C) to avoid the solid state transformation [18]. The as-solidified and as-annealed microstructures of the undercooled Fe–Cu alloy were examined using VEGAII XMH scanning electron microscopy (SEM). Composition was identified using VEGAII XMH energy-dispersive mode (EDS). Examination of the crystalline phase was conducted by Panalytical X'pert Pro type X-ray diffractometer (XRD).

3. Experimental results

Combined highly undercooled solidification with rapid quenching after recalescence, a homogeneous supersaturated granule grain was prepared. However, the as-formed single-phase equiaxed grains were not the final stabilized microstructure. Upon annealing at high temperatures, grain growth concurred with segregation of Cu atoms to GBs.

3.1. Formation of single-phase supersaturated granular grain

The as-solidified microstructure of single-phase supersaturated granular (with ΔT = 210 K) has been shown in Fig. 1. The composition of the alloy was determined to be 96 at.% Fe and 4 at.% Cu, with no detectable contaminations using SEM-EDS. From the analysis of EDS, the solute distribution in single grain was almost symmetrical, indicating that the solute segregation was suppressed, see Fig. 2.

Preparation of single-phase supersaturated granular grain in the Fe–4 at.% Cu immiscible alloy melt has been described in Ref. [4]. Herein, a concise description of two prerequisites was given which, from the side of solidification and solid-state transformation, influence the formation of single-phase supersaturated granular grain.

As mentioned in Ref. [4], analysis of dendrite growth should refer to nonlinear liquidus and solidus at high ΔT values. Accordingly, for undercooled Fe–Cu alloys, the extended dendrite growth model [19] (i.e. Eqs. (1)–(7) in Ref. [4]) incorporating non-linear liquidus and solidus, non-equilibrium solute diffusion, and non-equilibrium interface kinetics, is quite applicable to describe the solidification process quantitatively. With sufficiently high undercooling ($\Delta T \geq \Delta T(V_D) \approx 196$ K), the transition of $V - \Delta T$ relation from power law to linear growth as well as the partition-less solidification (i.e. absolute solute trapping) occurred thus providing one prerequisite for forming a homogeneous solid solution (see Fig. 4 in Ref. [4]).

The other prerequisite for forming a homogeneous solid solution is suppression of the dot substructure originating from δ/γ solid-state transformation. Previous research found that the dot substructure could be suppressed by rapid quenching immediately after recalescence [4]. Subjected to high cooling rate, the δ/γ transformation mode was changed from volume diffusion controlled transformation to interface controlled massive transformation [20,21], which can be suppressed by sufficiently high cooling rate.

3.2. Heat treatment of the as-solidified granular grains

Heat treatment was taken for the as-prepared single-phase supersaturated granular grains. The grain size observed by SEM is plotted in Fig. 3. Obvious grain growth occurred with the annealing time when annealing the samples at different temperatures and then tended to a stabilized value.

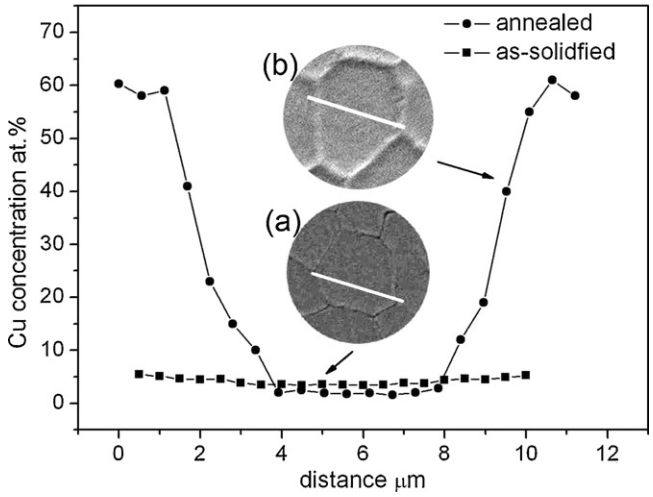

Fig. 2. Cu concentration profiles measured with EDS across the grains of the microstructures (lines in the insert micrograph). (a) As-solidified at ΔT = 210 K; (b) annealed at 800 °C for 60 min.

Fig. 4 shows the microstructures of the samples annealed at 600 °C and 800 °C, respectively. In all samples a white halo at the GBs was formed and the white halo tended to be thicker with increasing the annealing time. It could be resulted by a significant Cu segregation which could be evidenced by the analysis of SEM-EDS (Figs. 2 and 4). The XRD spectrum of the sample annealed at 800 °C for 60 min is plotted against the as-solidified sample in Fig. 5, where only α-Fe phase is evidenced. XRD confirmed that no secondary phases were present in any of samples including the sample annealed at 800 °C for 60 min. It was suggested that only Cu solute segregation led to the stabilized grain size and then established a metastable equilibrium state. Similar results could also be obtained in the samples annealed at 500 °C and 700 °C.

4. Thermo-kinetic grain growth model applicable for undercooled Fe–Cu alloy

4.1. Thermodynamic description

In 1992, Weissmüller [9] first presented a concept for the stabilization of nanocrystalline (NC) solids against grain growth by GB segregation. Later, an analogous analytical treatment was derived by Kirchheim [10] and Liu and Kirchheim [11] on the basis of Gibbs

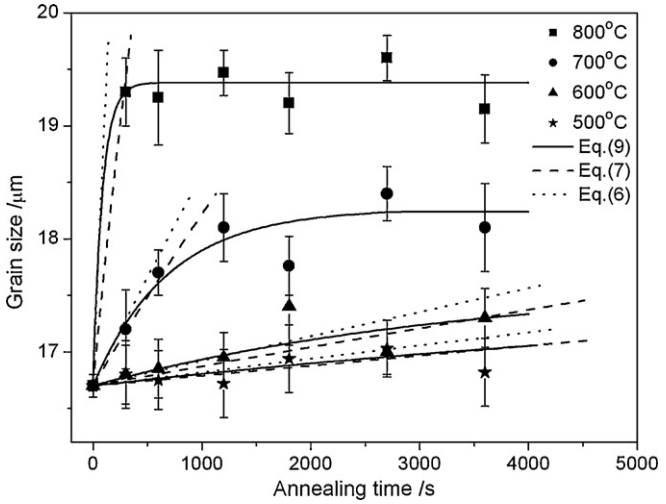

Fig. 3. Evolution of the average grain size with the annealing time for the Fe–4 at.% Cu alloy (ΔT = 210 K) annealed at different temperatures. The symbols are the experimental data annealed at 500, 600, 700 and 800 °C; the dotted, dashed and solid lines are calculated using Eq. (6) (the parabolic model), Eq. (7) (the pure kinetic model) and Eq. (9) (the thermo-kinetic model), respectively.

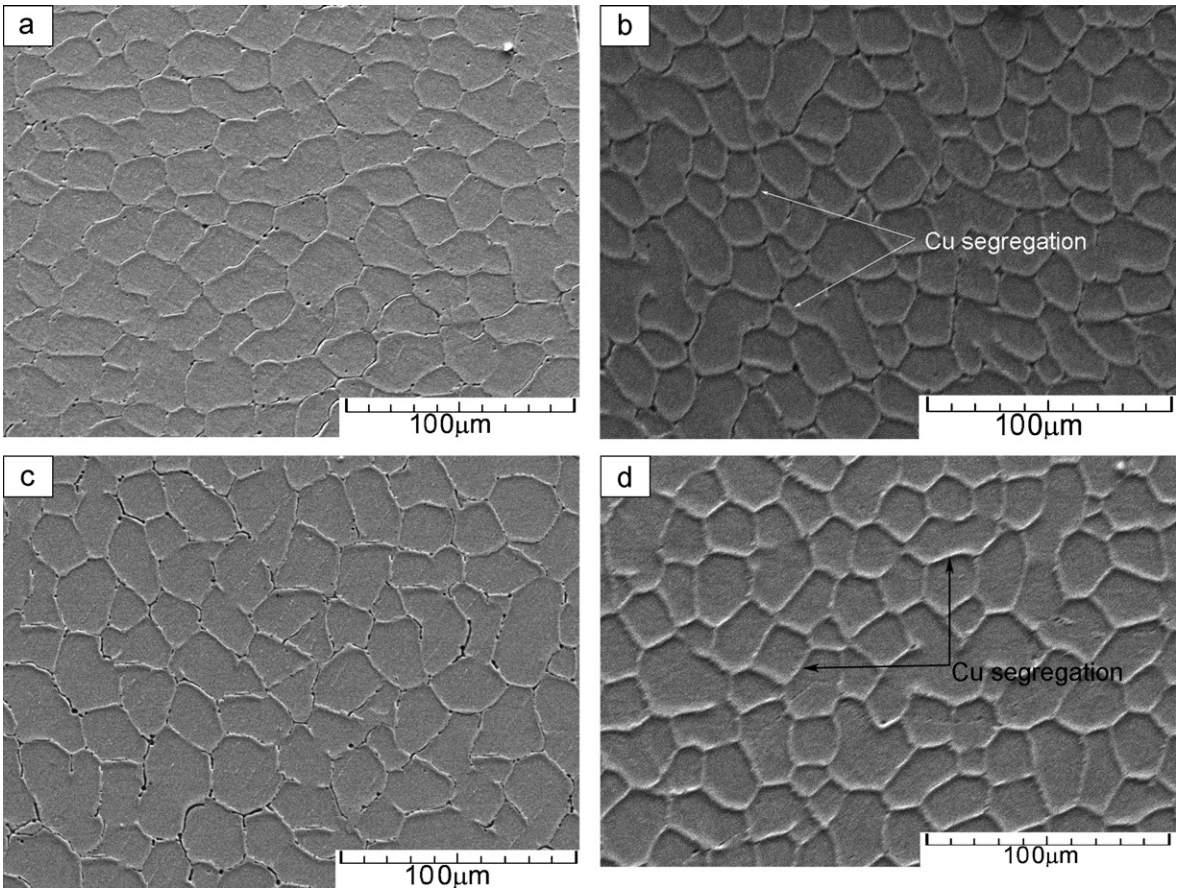

Fig. 4. Microstructure of the as-annealed single-phase supersaturated granular grains at different temperatures and annealing time. (a) 600 °C, 30 min; (b) 600 °C, 60 min; (c) 800 °C, 30 min; (d) 800 °C, 60 min.

adsorption equation [12],

$$\sigma_b = \sigma_0 - \Gamma_{b0}\left[RT\ \ln\left(x_0 - \frac{3\Gamma_b V_m}{D}\right) + \Delta H_{seg}\right] \quad (1)$$

where σ_0 is the GB energy for pure solvent, V_m the molar volume of the alloy, ΔH_{seg} the enthalpy change of segregation per mole of solute, x_0 the average concentration of the whole system, Γ_{b0} the saturated solute excess amount, Γ_b ($\leq\Gamma_{b0}$) is the solute excess amount at GBs.

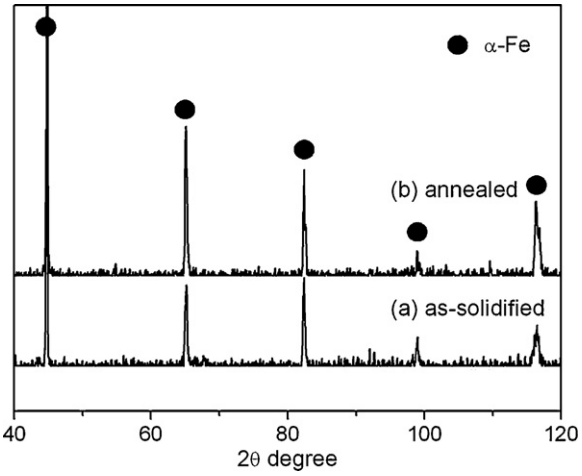

Fig. 5. XRD patterns for the as-solidified and the annealed single-phase supersaturated granular grains in undercooled Fe–4 at.% Cu alloy: (a) as-solidified at ΔT = 210 K; (b) annealed at 800 °C for 60 min.

It can be inferred from Eq. (1) that grain growth stops with Γ_b approaching Γ_{b0} as σ_b is close to zero. However, is the GB segregation saturated or not at the beginning of grain growth, i.e. the value of Γ_b must be lower than or equal to Γ_{b0}? Departing from Gibbs equation [12] and McLean's treatment for GB segregation [22], Gong et al. [17] categorized the state criterion of initial GB segregation as saturated GB segregation condition ($\Gamma_b/\Gamma_{b0} = 1$) and unsaturated GB segregation condition ($\Gamma_b/\Gamma_{b0} < 1$).

For $\Gamma_b/\Gamma_{b0} = 1$, according to the first order Taylor expansion, Eq. (1) can be rewritten as,

$$\sigma_b = \sigma_0 - \Gamma_{b0}(RT\ \ln x_0 + \Delta H_{seg}) + \frac{3RT\Gamma_{b0}^2 V_M}{x_0}\frac{1}{D} \quad (2)$$

For $\Gamma_b/\Gamma_{b0} < 1$, Eq. (1) can be rewritten as,

$$\sigma_b = \sigma_0 - \Gamma_{b0}(R_g T\ \ln x_0 + \Delta H_{seg}) + \frac{3\Gamma_{b0}RTV_m\Gamma_b}{x_0 D} \quad (3)$$

For strong segregating undercooled Fe–Cu system within microscale, a relation between Γ_b and D (see Appendix A) gives the GB excess amount as,

$$\Gamma_b \approx x_0\rho\left(\frac{D}{6} + \Delta\right) \quad (4)$$

Substitution of Eq. (4) into Eq. (3) leads to,

$$\sigma_b = \sigma_0 - \Gamma_{b0}\left[RT\left(\ln\ x_0 - \frac{V_m\rho}{2}\right) + \Delta H_{seg}\right] + 3\Gamma_{b0}RTV_m\rho\Delta\frac{1}{D} \quad (5)$$

Apparently, Eq. (5) is analogous to $\sigma_b = \sigma_1 - \sigma_2 D$ from Chen et al. [14] and the difference between Eq. (5) and that from Chen et al. lies in whether the effect of the configurational entropy is considered

or not. Although the model proposed by Chen et al. [14] was applicable for grain growth of nano-scale materials, the present model has been extended to undercooled Fe–Cu alloy within micro-scale according to the "surface segregation effect" [22–25] (see Section 5.1 and Appendix A). In all samples a white halo at the GBs was formed and the white halo tended to be thicker. It could be resulted by a significant Cu segregation which could be evidenced by the analysis of SEM-EDS (Figs. 2 and 4).

Note that GB concentration increased with the increase of annealing time (see Figs. 2 and 4). In other words, GB excess amount Γ_b increased gradually and tended to the saturated value Γ_{b0}. This highlights the fact that the assumption of the initial unsaturated GB segregation condition ($\Gamma_b/\Gamma_{b0} < 1$ [17]) is suitable for undercooled Fe–Cu system; for this case Eq. (5) is preferable.

4.2. Kinetic description

The driving force for GB migration arises from its curvature. A classical theory for grain growth [6] deduces that the growth rate, V (i.e. dD/dt) is related to the interface mobility, M, and the driving force $P(V)$,

$$V = MP(V) = M\frac{\sigma_b}{D} \Rightarrow D^2 - D_0^2 = 2M\sigma_b t \tag{6}$$

This classical parabolic model is precisely applicable to high-purity, single-phase materials. In general, both M and $P(V)$ are functions of state variables such as T and x_0 [26]. According to Rabkin [27], the solute drag term P_S is introduced to model the stagnation of growth in most real materials. Regarding the dependence of solute drag on GB concentration (X_b) and velocity (V), the drag term should be given as $P_S = \beta D \times dD/dt$ [8], so that the model is given as,

$$P(V) = P_S + \frac{V}{M} \Rightarrow \left(\frac{1}{M} + \beta D\right)\frac{dD}{dt} = \frac{\sigma_b}{D} \Rightarrow (D^2 - D_0^2) + \frac{2M\beta}{3}(D^3 - D_0^3) = 2M\sigma_b t \tag{7}$$

with β as a constant. As compared to the previous model from Michels et al. [7], an integrated effect of solute drag due to X_b and V is thus expected as a more rational manner for the stabilization.

4.3. Thermo-kinetic description

With reference to [14,28], as the GB area decreases upon grain growth, the segregated solute atoms must be re-distributed throughout the GB network. Meanwhile, the activation energy for GB diffusion is increased, accompanied with a decreased GB diffusion coefficient, D_b. From Borisov's equation [16], once D_b and the lattice diffusion coefficient D_l become equivalent, a thermodynamic metastable equilibrium state (i.e. $\sigma_b = 0$) results. Thus, incorporation of the GB energy decreasing with GB segregation into the parabolic kinetics is physically practicable [13–17]. Analogous to the treatment of Ref. [14], a substitution of Eq. (5) into (7) leads to,

$$\int_{D_0}^{D} \frac{D(1/M + \beta D)}{\sigma_1 + (\sigma_2/D)}\,dD = \int_0^t dt \tag{8}$$

with $\sigma_1 = \sigma_0 - \Gamma_{b0}(RT(\ln x_0 - V_m\rho/2) + \Delta H_{seg})$, $\sigma_2 = 3\Gamma_{b0}RTV_m\rho\Delta$, and the boundary condition as: $t = 0$, $D = D_0$ and $t = t$, $D = D(t)$.

Integrating Eq. (8) leads to an evolution of grain size with time,

$$\left\{\frac{\beta}{3\sigma_1}\left[\left(D + \frac{\sigma_2}{\sigma_1}\right)^3 - \left(D_0 + \frac{\sigma_2}{\sigma_1}\right)^3\right] + \left(\frac{1}{2\sigma_1 M} - \frac{3}{2}\frac{\beta\sigma_2}{\sigma_1^2}\right)\left[\left(D + \frac{\sigma_2}{\sigma_1}\right)^2 - \left(D_0 + \frac{\sigma_2}{\sigma_1}\right)^2\right] + \left(\frac{3\beta\sigma_2^2}{\sigma_1^3} - \frac{2\sigma_2}{M\sigma_1^2}\right)(D - D_0) + \left(\frac{\sigma_2^2}{\sigma_1^3 M} - \frac{\beta\sigma_2^3}{\sigma_1^4}\right) \ln\frac{D + (\sigma_2/\sigma_1)}{D_0 + (\sigma_2/\sigma_1)}\right\} = t \tag{9}$$

with D_0 as the initial average grain size. Eq. (9) is defined as the model for grain growth considering the mixed effect due to kinetics and thermodynamics. The equation gives the evolution of the average grain size with the annealing time.

5. Model application in grain growth of the as-prepared granular grains

The as-formed equiaxed grains are not the final stabilized microstructure. Upon annealing at high temperatures, grain growth concurs with segregation of Cu atoms to GBs.

5.1. Validity of the thermo-kinetic model applied to undercooled Fe–Cu alloy

It should be noted that the above models (cf. Kirchheim's [10], Chen et al.'s [14,15] and Gong et al.'s [17]) are truely applied to nano-scale grain growth, however, for the undercooled Fe–Cu system, the real grain size and GB thickness are in micro-scale. Since Fe–Cu system has a large positive enthalpy of mixing [29], the decomposition tendency of the as-prepared grains at elevated temperatures is very strong. As for a grain, because the broken bonds in GBs are more than in the bulk, and moreover, the cohesive energy of Cu is 3.55 eV, which is smaller than that of Fe (4.25 eV), GB segregation of Cu must occur.

In the case of the solute segregation in nano-scale, the GB segregation should conform to the saturated equivalent monolayer segregation [22], which occurs at the very surface of the GB (i.e. $\Gamma_{b0} \approx \delta\rho X_{b0}$, with X_{b0} as the saturated GB content and GB thickness $\delta \approx 3 \times 10^{-10}$ m [23]). However, in binary alloys of two transition metals, such as Fe and Cu [24], the real segregation can build up to several equivalent monatomic layers, i.e. "surface segregation". Therefore, the surface segregation of undercooled Fe–Cu alloy (in micro-scale) takes place at the actual segregation sites (i.e. $\Gamma_b \approx \Delta\rho X_b$, with X_b as the GB content and $\Delta \approx 10^{-7}$ m the actual GB thickness [23], Fig. 4) averaged in the whole GB zone.

In conclusion, the present thermo-kinetic model is more rational for the analysis of grain growth in micro-scale undercooled Fe–Cu alloy with strong segregating effect. Under specific limitations Eq. (9) is reduced to previous models.

(i) If σ_b is considered as a constant value (i.e. GB energy effect is neglected), Eq. (9) will be reduced to pure kinetic model (Eq. (7)), i.e. Rabkin's model [27].
(ii) If the GB energy effect is solely considered, Eq. (9) will reduce to pure thermodynamic model (Eq. (5)) which is consistent with the illustration by Kirchheim's [10] and Krill's model [26].

5.2. Model calculations

The Fe–Cu system has an equilibrium solubility limit of 1.9 at.% Cu in Fe at 850 °C and at lower temperatures the equilibrium solubility is reduced further to about 0 [18]. Therefore, the thermo-kinetic model is quite applicable for micro-scale grain growth in undercooled Fe–Cu alloy with strong segregating tendency. The parabolic model (Eq. (6)), pure kinetic model (Eq. (7)), pure thermodynamic model (Eq. (5)) and thermo-kinetic model (Eq. (9)) are applied to analysis the mechanism of grain growth and solute segregation.

Table 1
Values for parameters used in the calculations in terms of Eq. (9).

Parameters	Temperature/°C			
	500	600	700	800
GB energy (σ_0) J/m^2	0.79	0.79	0.79	0.79
Saturated excess (Γ_{b0}) at.%	2.9×10^{-5}	2.9×10^{-5}	2.9×10^{-5}	2.9×10^{-5}
Actual GB thickness (Δ) μm	0.1	0.1	0.1	0.1
Enthalpy change (ΔH_{seg}) kJ/mol	49.15	52.29	55.39	58.49
Mobility (M) m^4/J s	1.9×10^{-11}	4.9×10^{-11}	2.1×10^{-10}	2.1×10^{-9}

The parabolic model (Eq. (6) with constant σ_b and $\beta = 0$), the pure kinetic model (Eq. (7) with σ_b as constant and $\beta = 1/MD_0$ [27]) and the thermo-kinetic model (Eq. (9)) with $\beta = 1/M$[1]) were applied to fit the experimental data, see Fig. 3. The parameters are shown in Table 1. From Fig. 3, the classical parabolic model (dotted lines) cannot be brought into agreement with the experimental data. The pure kinetic model could give a fit description at 500 °C and 600 °C and the initial stage at 700 °C and 800 °C. It is evidenced that although the rate of grain growth is partially inhibited due to the solute drag effect, the pure kinetic model still could not give a satisfied description. A good fit to the experimental data is only obtained using the present thermo-kinetic model (Eq. (9)) due to the introduction of the mixed effect of GB energy and solute drag.

According to Martin and Doherty [30], the surface free energy for pure Fe is 2.2 J/m^2 and thus the GB energy σ_0 for pure Fe is approximately 1/3 of the surface free energy (≈0.73 J/m^2) [26,31]. In fact, both pulsed laser deposition and undercooled solidification are all non-equilibrium processes. Moreover, the exact value of σ_0 has not been determined, but only roughly estimated value 0.7–0.8 J/m^2. σ_0 was chosen to be 0.79 J/m^2 according to the analysis of Liu for NC Fe–Ag alloy through pulsed laser deposition [32]. Upon fitting, ΔH_{seg}, M and Γ_{b0} act as the fitting parameters. ΔH_{seg} was fitted as 49–59 kJ/mol (Table 1), which was close to the roughly estimated value 40 kJ/mol using $\Delta H_{seg} \approx RT \ln x_{op} - (10 \pm 6)$ [10] with $x_{op} \approx 1.9$ at.% Cu in Fe (at 850 °C) as the terminal solute solubility [18].

6. Discussions

In Section 3, the formation of the as-prepared single-phase granular grains and the subsequent grain growth and solute segregation were described for undercooled Fe–4 at.% Cu alloys. At high temperatures the grains grew rapidly during a relatively short period of time and then the grain size did not change essentially any more with time. On this basis, the characteristic time and possible controlled-mechanism of grain growth will be discussed in this part.

As described by Refs. [13–15], the evolution of grain size with time is a kinetic process controlled by thermodynamic factor (reduced GB energy with grain growth). That is to say, the thermodynamic factor or kinetic factor may play the main role at different periods of annealing time in the whole thermo-kinetic process. Obviously, the rapid increase of grain size is a kinetic process, and the final period is a thermodynamic stabilized stage. It could be further evidenced by the model calculations that the pure kinetic model (Eq. (7)) was used to describe the rapid increase of grain size at initial stage, and that the stabilized grain size (D^*) can be determined using pure thermodynamic model (Eq. (5)) when $\sigma_b = 0$. The whole process of grain size evolution could be rationally categorized as three stages: initial kinetic stage, middle mixed stage and final thermodynamic stage. Consequently, there must be two characteristic annealing time that could determine the transition from kinetic process to thermodynamic process quantitatively. However, how can the characteristic time be determined physically?

Three theoretical models of grain growth (pure kinetic model (Eq. (7)), pure thermodynamic model (Eq. (5)) and thermo-kinetic model (Eq. (9)) was compared in Fig. 6. Both Eqs. (7) and (9) could describe the rapid increase of grain size at the period of $t \le t_1$ well. It can be concluded that the same mechanism (i.e. mainly kinetic-controlled mechanism) controlled the evolution of grain size at $t \le t_1$. However, the grain size $D_{kinetic}$ determined by Eq. (7) increases continuously and exceeds the grain size $D_{thermo\text{-}kinetic}$ determined by Eq. (9) at $t > t_1$. That is to say, the controlled-mechanism of grain growth changes from kinetic-controlled mechanism to mixed mechanism of kinetics and

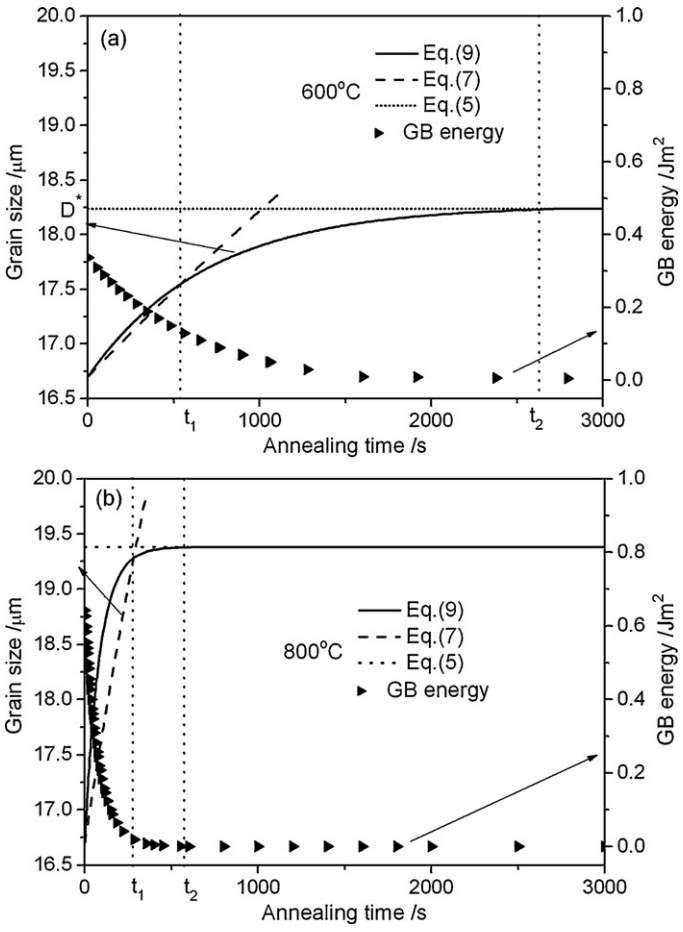

Fig. 6. Evolution of the average grain size and GB energy with the annealing time annealed at 600 and 800 °C. Then GB energy is calculated using Eq. (13) (see Fig. 8). Two critical times were determined. t_1: $D_{kinetic}$ determined by Eq. (7) equals to $D_{thermo\text{-}kinetic}$ determined by Eq. (9); t_2: $D_{thermo\text{-}kinetic}$ tends to D^* when σ_b tends to 0 (D^* is determined using Eq. (5) when $\sigma_b = 0$).

[1] The selection of constant β will not influence the model analysis. For example, $\beta = \sigma_b/D^2_{max}$ (with D_{max} as the limiting grain size) was determined by Michels et al. [7]; Rabkin [27] gave a hypothetical value $\beta = 1/MD_0$. Regarding the complexity of calculation depending on β, $\beta = \sigma_2/M$ was assumed by Chen et al. [14]. In order to derive an analytical model, $\beta = 1/M$ was assumed in the present case.

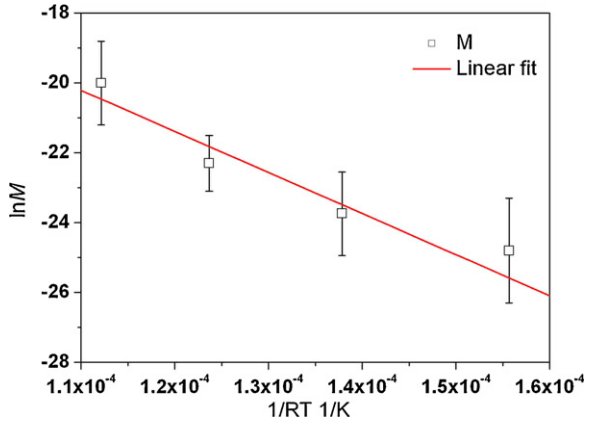

Fig. 7. Arrhenius plot of the GB mobility M against the annealing temperature calculated using Eq. (11). The activation energy $Q = 117.6$ kJ/mol was given.

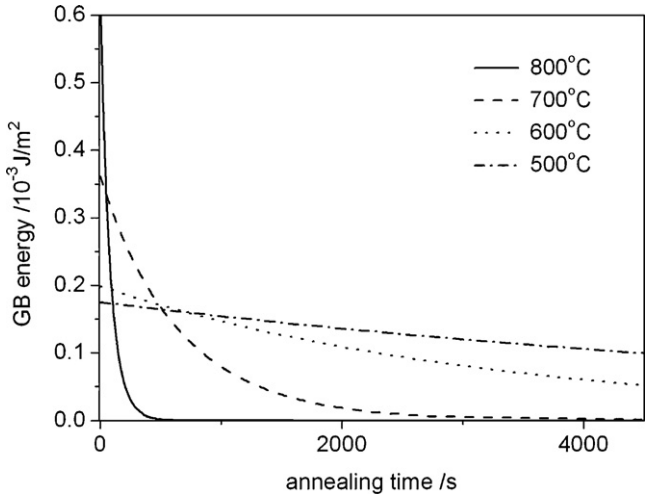

Fig. 8. Evolution of the GB energy with the annealing time at different temperatures calculated using Eq. (13). Obviously, the GB energy infinitely approaches zero with annealing time.

thermodynamics because of the incorporation of GB energy effect at t_1. Therefore, t_1 could be determined as an important characteristic time.

On the other hand, both Eq. (5) (when $\sigma_b = 0$) and Eq. (9) could describe the stabilized grain size at the period of $t \geq t_2$ well. As shown by Fig. 6, $D_{thermo\text{-}kinetic}$ tends to D^* because of the incorporation of GB energy effect and almost reaches it at t_2 ($\sigma_b = 0$). Therefore, t_2 could be determined as another characteristic time which forecasts a transition from mixed controlled growth to purely thermodynamic-controlled growth.

Until now, in comparison of Eqs. (5), (7) and (9), the two critical annealing time could be determined,

$$t = \begin{cases} t_1 & D_{kinetic} = D_{thermo\text{-}kinetic} \\ t_2 & D \approx D^* \quad (\sigma_b \approx 0) \end{cases} \tag{10}$$

With regard to the two characteristic time, the overall process of grain growth can be categorized as follows:

(1) Mainly kinetic-controlled growth ($t \leq t_1$)

The kinetic approach suggests that mobility M plays an important role in grain growth. The GB mobility, M can be expressed in an Arrhenius-type equation [7],

$$M = M_0 \ \exp\left(-\frac{Q}{RT}\right) \tag{11}$$

with R as the gas constant, M_0 a constant and Q the activation energy for isothermal grain growth. Fit of Eq. (11) to the calculated value of M (Table 1) a straight line (Fig. 7) was resulted, and a constant activation energy $Q = 117.6$ kJ/mol can be deduced from the slope of the line, which is closer to the value of 125 kJ/mol for GB diffusion in NC Fe produced by high energy ball milling [33]. Meanwhile, the value is slightly lower than the activation energy for GB diffusion of 174 kJ/mol in Fe [34]. According to the detection of Ref. [33], the grain growth of undercooled Fe–Cu alloy is controlled by GB diffusion. Therefore, the low activation energy ($Q = 117.6$ kJ/mol) and high GB mobility M (i.e. kinetic process) may play an important role on the rapid increase of grain size at the initial stage.

(2) A transition from kinetic-controlled growth to thermodynamic-controlled growth ($t_1 < t < t_2$)

A quasi-quantitative analysis for the effect of GB energy on the grain growth is given by differentiation of Eq. (5) over t,

$$\frac{d\sigma_b}{dt} = \frac{\sigma_2}{D^2}\frac{dD}{dt} \tag{12}$$

In combination with Eqs. (5) and (7) with $\beta = 1/M$ (see Section 5.2) leads to,

$$\int_{\sigma_1}^{\sigma_b} \frac{\sigma_1 + \sigma_2 - \sigma_b}{(\sigma_1 - \sigma_b)^4 \sigma_b}\, d\sigma_b = \frac{M}{\sigma_2^2}\int_0^t dt \tag{13}$$

The evolution of GB energy with the annealing time for as-prepared Fe–Cu granular grains is calculated (Figs. 6 and 8) using the parameters listed in Table 1. As shown in Fig. 8, σ_b decreases with grain growth. When $t > t_1$, GB energy decreases rapidly and tends to zero at $t \sim t_2$ thus the growth rate of $D_{thermo\text{-}kinetic}$ decreases due to the GB energy effect. Conceptually, the GB energy is reduced with solute segregation since solute atoms can effectively reduce elastic mismatch strains in the GBs [35]. As for Fe–Cu alloys, the extremely low-solid-solubility of Cu in Fe [18] usually implies that these systems with extensive Cu segregation (Figs. 2 and 4). The effect of thermodynamics increases with solute segregation. Therefore, at ranges $t_1 < t < t_2$, it is a transition of controlled-mechanism from mainly kinetic mechanism (i.e. GB diffusion) to main thermodynamic mechanism (i.e. reduction of GB energy with solute segregation).

(3) Purely thermodynamic-controlled growth ($t \geq t_2$)

Obviously, the migration of GB should be rapid due to the low activation energy ($Q = 117.6$ kJ/mol) and high GB mobility M. Unfortunately, only rapid increase of grain size occurs at $t \leq t_1$, especially at 700 and 800 °C. Once $t \geq t_2$, $\sigma_b \sim 0$, the stabilized size D^* tends (see Fig. 6),

$$D^* = \frac{3\Gamma_{b0}RTV_m\rho\Delta}{\Gamma_{b0}\left[RT(\ln x_0 - (V_m\rho/2)) + \Delta H_{seg}\right] - \sigma_0} \tag{14}$$

Therefore, with the decrease of GB energy, i.e. the decrease of driving force of GB migration, the thermodynamic effect is a key stabilized mechanism at the final stage in undercooled Fe–Cu alloys.

7. Conclusions

An analysis of thermal stabilized mechanism of single-phase supersaturated granular grains in the undercooled Fe–4 at.% Cu immiscible alloy was presented. The main conclusions can be summarized as follows:

1. The thermo-kinetic model proposed by Chen et al. applicable for nano-scale materials was extended to be used in micro-scale undercooled Fe–4 at.% Cu alloy granular grains. The model was consistent with the experimental results.
2. In comparison of pure kinetic model, pure thermodynamic model and the extended thermo-kinetic model, two characteristic time (t_1, t_2) were determined.
3. The controlled-mechanism of grain growth process in undercooled Fe–Cu alloy was proposed, i.e. a mainly kinetic-controlled process ($t \le t_1$), a transition from kinetic-mechanism to thermodynamic-mechanism ($t_1 < t < t_2$) and purely thermodynamic-controlled process ($t \ge t_2$).

Acknowledgements

The authors are grateful to the Fundamental Research Funds for the Central Universities (2010QNA06), the fund of the State Key Laboratory of Solidification Processing in NWPU (SKLSP201119) and the Natural Science Foundation of the Education Department of Jiangsu province (09KJB430004).

Appendix A. Estimating the solute excess amount of undercooled Fe–Cu alloy

As for undercooled Fe–Cu immiscible alloys, the GB may be represented as a region having volume $V_b = A\Delta$ with A as the GB area and Δ the GB thickness. The concentration of solute in this region is $X_b = \xi X_\alpha$, ξ is a distribution coefficient. A simple mass balance calculation can be adopted to predict the overall concentration of solute atoms in a given sample, x_0 [7,36],

$$x_0 = X_\alpha \frac{V_\alpha}{V_0} + X_b \frac{V_b}{V_0} \tag{A1}$$

where V_α represents the volumes of the matrix, $V_0 = V_\alpha + V_b$ the entire sample volume.

The fraction of GB volume follows (assuming spherical grains of diameter D) [37],

$$f = \frac{V_b}{V_\alpha} = \frac{((D/2)+\Delta)^3 - (D/2)^3}{(D/2)^3} \approx \frac{6\Delta}{D} \tag{A2}$$

then

$$x_0 = X_b \left[\frac{1}{\xi} + \frac{f}{1+f}\left(1 - \frac{1}{\xi}\right)\right] \tag{A3}$$

Generally, the GB segregation should conform to the saturated equivalent monolayer segregation [22], i.e. the monolayer segregation occurs at the very surface of the GB (GB thickness $\delta \approx 3 \times 10^{-10}$ m). However, the real segregation can build up to several equivalent monatomic layers in binary alloys of two transition metals, such as Fe, Ni, Cu, Ag, and Au [24]. This is called "surface segregation". The surface segregation takes place at the actual segregation sites (with $\Delta \approx 10^{-7}$ m as the actual GB thickness, Fig. 4) averaged in the whole GB zone. Generally, the grain size of undercooled Fe–Cu alloys between 10 μm and 100 μm, and Δ between 0.1 and 1 μm ($\Delta \approx 0.1$ μm [23]). Since Fe–Cu system has a large positive enthalpy of mixing [35], the decomposition tendency of the as-prepared single-phase solid solution at elevated temperatures is strong. Therefore, for strongly segregating Fe–Cu systems, it can be reasonably assumed $\xi \gg 1$. Then combining Eqs. (A1)–(A3) gives,

$$X_b - X_\alpha = X_b \frac{\xi - 1}{\xi} = \frac{x_0(\xi - 1)}{1 + (f/(1+f))(\xi - 1)} = x_0 \frac{(1+f)}{f} \tag{A4}$$

Γ_b is the solute excess amount at GBs, which can be expressed as [38],

$$\Gamma_b = \Delta(\rho_b X_b - \rho_\alpha X_\alpha) \tag{A5}$$

where ρ_b and ρ_α are the density in the GB and in the matrix, respectively. Suppose the mean density of the GBs and of the whole system are equal to that of the dilute alloy, i.e. $\rho_b \approx \rho_\alpha \approx \rho$, the solute excess amount at GBs can be given as,

$$\Gamma_b = \Delta\rho(X_b - X_\alpha) \approx x_0 \rho \left(\frac{D}{6} + \Delta\right) \tag{A6}$$

As for undercooled Fe–Cu alloys, Γ_b in Eq. (A6), standing for the actual segregation sites averaged in the whole GB, whereas, Γ_{b0} in Eq. (9), corresponding to the maximum sites for the first equivalent monolayer segregation, can be expressed as $\delta\rho X_{b0}$, where δ ($\approx 3 \times 10^{-10}$ m) cannot be considered as the real GB width, but as the monatomic thickness. That is to say, the saturated equivalent monolayer segregation, X_{b0}, occurs at the very surface of the GB ($\approx 3 \times 10^{-10}$ m), whereas the bulk segregation, X_b takes place at the actual segregation sites averaged in the whole GB zone ($\approx 1 \times 10^{-7}$ m), with $X_b \ll X_{b0}$ [23].

References

[1] M.N. Baibich, J.M. Broto, A. Fert, F. Nguyen van Dau, F. Petroff, P. Etienne, G. Creuzert, A. Friederich, J. Chazeles, Phys. Rev. Lett. 61 (1989) 2472–2475.
[2] J. Wang, G. Xiao, Phys. Rev. B 49 (1994) 3982–3996.
[3] M. El Ghannami, C. Gómez-Polo, G. Rivero, A. Hemando, Europhys. Lett. 26 (1994) 701–704.
[4] Z. Chen, F. Liu, H.F. Wang, W. Yang, G.C. Yang, Y.H. Zhou, J. Cryst. Growth 310 (2008) 5385–5391.
[5] D.M. Herlach, Mater. Sci. Eng. R 12 (1994) 177–272.
[6] J.E. Burke, Trans. Metall. Soc. AIME 175 (1949) 73–91.
[7] A. Michels, C.E. Krill, H. Ehrhardt, R. Birringer, D.T. Wu, Acta Mater. 47 (1999) 2143–2152.
[8] J.W. Cahn, Acta Metall. 10 (1962) 789–798.
[9] J. Weissmüller, Nanostruct. Mater. 3 (1993) 261–272.
[10] R. Kirchheim, Acta Mater. 50 (2002) 413–419.
[11] F. Liu, R. Kirchheim, J. Cryst. Growth 264 (2004) 385–391.
[12] J.W. Gibbs, Trans. Conn. Acad. III 108 (1876);
J.W. Gibbs, Trans. Conn. Acad. III 343 (1878);
J.W. Gibbs, The Collected Works of J.W. Gibbs, vol. 1, Longmans, Green and Co., New York, 1928, pp. 55–354.
[13] K. Zhang, Z. Chen, F. Liu, G.C. Yang, J. Alloys Compd. 501 (2010) L4–L7.
[14] Z. Chen, F. Liu, H.F. Wang, W. Yang, G.C. Yang, Y.H. Zhou, Acta Mater. 57 (5) (2009) 1466–1475.
[15] Z. Chen, F. Liu, W. Yang, H.F. Wang, G.C. Yang, Y.H. Zhou, J. Alloys Compd. 475 (2009) 893–897.
[16] V.T. Borisov, V.M. Golikov, G.V. Scherbedinskiy, Fiz. Metal. Metall. 17 (1964) 80–85.
[17] M.M. Gong, F. Liu, K. Zhang, Scripta Mater. 63 (2010) 989–992.
[18] H. Okamoto, Phase Diagrams of Binary Iron Alloys, ASM International, Materials Park, OH, 1993, pp. 41–47, 131–137.
[19] H.F. Wang, F. Liu, Z. Chen, G.C. Yang, Y.H. Zhou, Acta Mater. 55 (2007) 497–506.
[20] J. Christian, The Theory of Transformation in Metals and Alloys, Pergamon Press, Oxford, 1965.
[21] F. Liu, F. Sommer, C. Bos, E.J. Mittemeijer, Int. Mater. Rev. 52 (2007) 193–212.
[22] D. Mclean, Grain Boundaries in Metals, Oxford University Press, Oxford, 1957.
[23] F. Liu, G.C. Yang, R. Kirchheim, J. Cryst. Growth 264 (2004) 392–399.
[24] E.D. Hondros, M.P. Seah, Metall. Trans. A 8A (1977) 1363–1371.
[25] Z. Chen, F. Liu, K. Zhang, Y.Z. Ma, G.C. Yang, Y.H. Zhou, J. Cryst. Growth 313 (2010) 81–93.
[26] C.E. Krill, H. Ehrhardt, R. Birringer, Z. Metallkd. 96 (2005) 1134–1141.
[27] E. Rabkin, Scripta Mater. 42 (2000) 1199–1206.
[28] T.D. Xu, B.Y. Cheng, Prog. Mater. Sci. 49 (2004) 109–208.
[29] A.K. Niessen, F.R. De Boer, R. Boom, CALPHAD 7 (1983) 51–70.
[30] J.W. Martin, R.D. Doherty, Stability of Microstructure in Metallic Systems, Cambridge University Press, Cambridge, 1976, p. 159.
[31] Kris##A. Darling, R.N. Chan, P.Z. Wong, J.E. Semones, R.O. Scattergood, C.C. Koch, Scripta Mater. 59 (2008) 530–533.
[32] F. Liu, Mater. Lett. 59 (2005) 1458–1462.
[33] T.R. Malow, C.C. Koch, Acta Mater. 45 (1997) 2177–2186.
[34] Smithells Metals Reference Book, 7th edn, Butterworth-Heineman, London, 1992, pp. 13-1–13-119.
[35] M.P. Seah, J. Phys. 10 (1980) 1043–1046.
[36] R.J. Brook, Scripta Metall. 2 (1968) 375–378.
[37] B. Färber, E. Cadel, A. Menand, G. Schmitz, R. Kirchheim, Acta Mater. 48 (2000) 789–796.
[38] G. Gottstein, L.S. Shvindlerman, Grain Boundary Migration in Metals, Thermodynamics, Kinetics, Applications, CRC Press, 1999.